Cell Reports, Volume *37*

Supplemental information

Potent neutralization of SARS-CoV-2 variants of concern by an antibody with an uncommon genetic signature and structural mode of spike recognition

Kevin J. Kramer, Nicole V. Johnson, Andrea R. Shiakolas, Naveenchandra Suryadevara, Sivakumar Periasamy, Nagarajan Raju, Jazmean K. Williams, Daniel Wrapp, Seth J. Zost, Lauren M. Walker, Steven C. Wall, Clinton M. Holt, Ching-Lin Hsieh, Rachel E. Sutton, Ariana Paulo, Rachel S. Nargi, Edgar Davidson, Benjamin J. Doranz, James E. Crowe Jr., Alexander Bukreyev, Robert H. Carnahan, Jason S. McLellan, and Ivelin S. Georgiev

Supplemental Figure 1

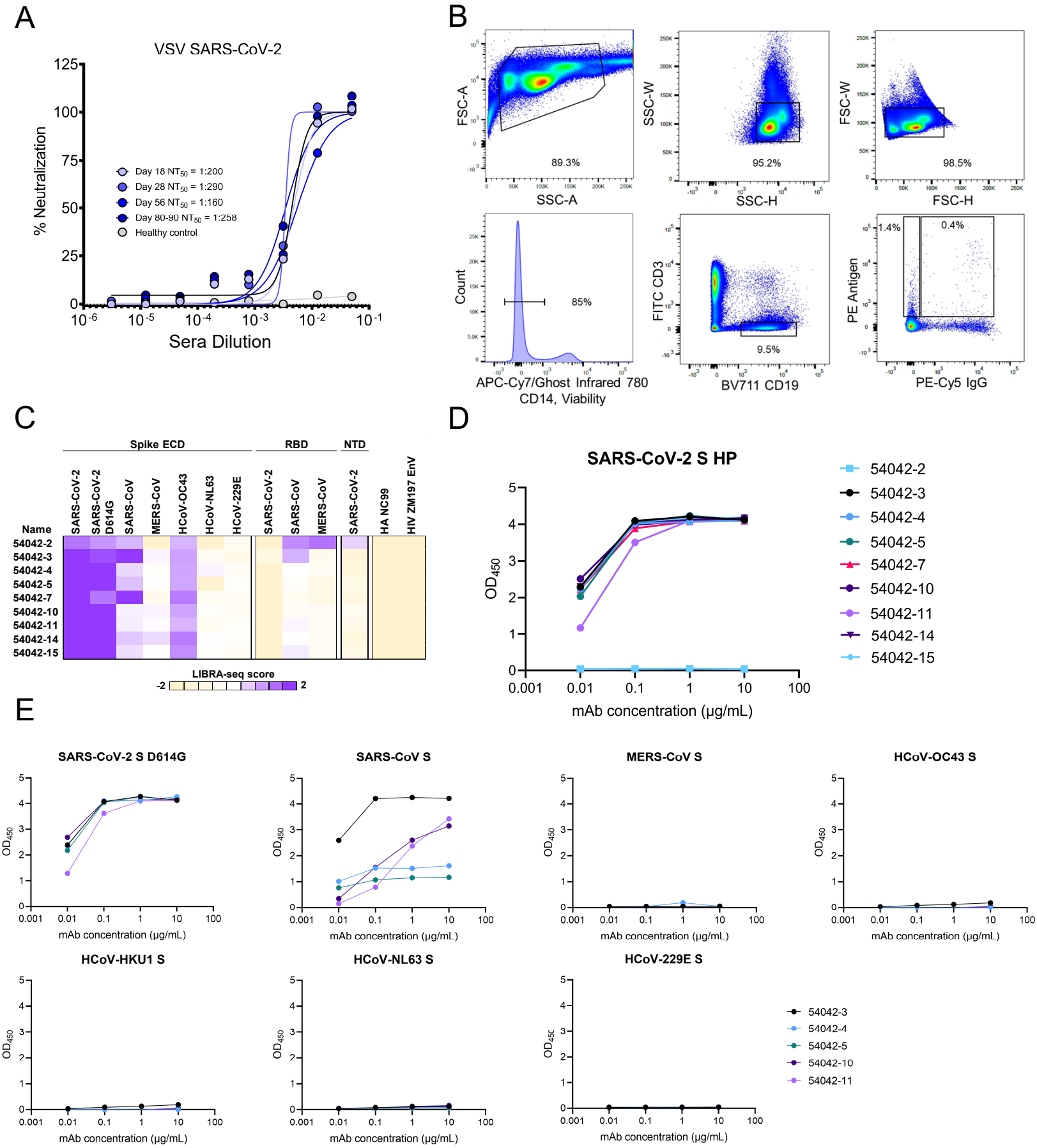

Supplemental Figure 1: Identification and characterization of SARS-CoV-2 neutralizing antibodies isolated using LIBRA-seq, related to Figure 1.

(A) VSV SARS-CoV-2 neutralization capacity of serum is displayed from time points at day 18, day 28, day 56, and days 80-90 post-COVID-19 infection. Neutralization was performed in single technical conditions with 1 biological replicate.

(B) Gating scheme for fluorescent-activated cell sorting of recovered COVID-19 individual. Cells were stained with Ghost Red 780 (viability), CD14-APC-Cy7, CD3-FITC, CD19-BV711, and IgG-PE-Cy5 along with a DNA-barcoded antigen screening library. To detect antigen-positive B cells, cells were washed and treated with a streptavidin-PE secondary stain. Gates as drawn are based on gates used during the sort, and percentages from the sort are listed.

(C) LIBRA-seq scores for SARS-CoV-2 S, SARS-CoV-2 S D614G, SARS-CoV S, MERS-CoV S, HCoV-OC43 S, HCoV-229E S, HCoV-NL63 S, SARS-CoV-2 RBD, SARS-CoV RBD, and MERS-CoV RBD, as well as negative-control antigens ZM197 Env and hemagglutinin (HA) NC99 are shown. LIBRA-seq scores for each antigen are displayed as a heatmap with a LIBRA-seq score of -2 displayed as light yellow, 0 as white, and 2 in purple; in this heatmap, scores lower or higher than that range are shown as -2 and 2, respectively.

(D) ELISA binding data of candidate antibodies identified by LIBRA-seq against SARS-CoV-2 S HP. The optical density at 450 nm (y-axis) is depicted as a function of antibody concentration (x-axis). ELISAs were performed in single technical conditions with 1 biological replicate.

(E) ELISA binding data of the antibodies that displayed neutralization in the high-throughput VSV SARS-CoV-2 RTCA (**Figure 1B**) for the antigens SARS-CoV-2 S D614G, SARS-CoV S, MERS-CoV S, HCoV-OC43 S, HCoV-HKU1 S, HCoV-NL63 S, and HCoV-229E S. The optical density at 450 nm (y-axis) is depicted as a function of antibody concentration (x-axis). ELISAs were performed in single technical conditions with 1 biological replicate.

Supplemental Figure 2

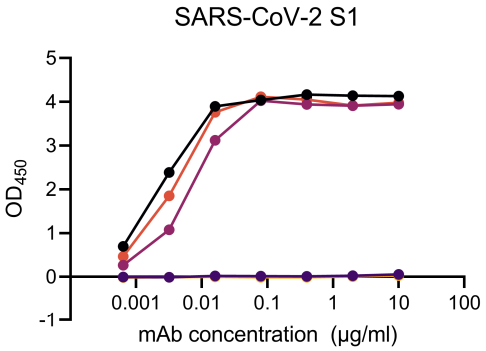

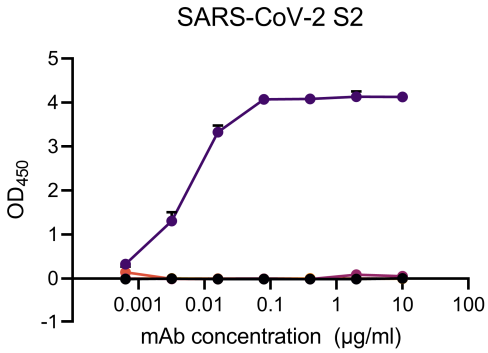

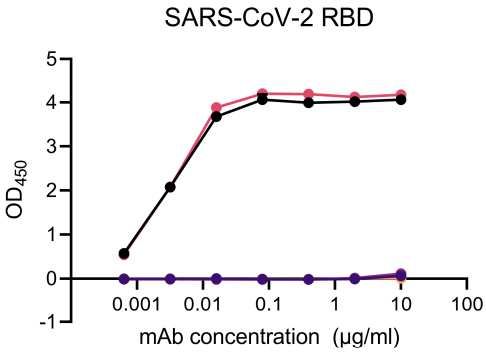

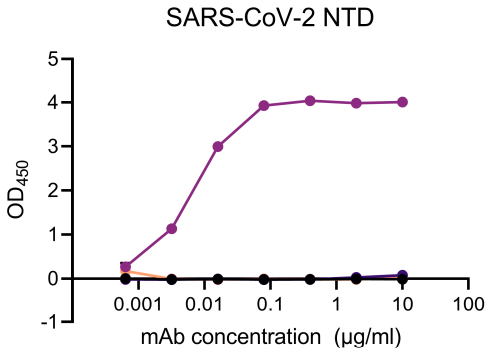

Supplemental Figure 2: Epitope mapping of antibody 54042-4 to SARS-CoV-2 subunit domains, related to Figure 2.

ELISA binding data against SARS-CoV-2 subdomains RBD, NTD, S1, and S2 are shown. CR3022 was used as a positive control RBD-directed antibody (Yuan et al., 2020a) whereas 46472-4 and 46472-6 antibodies were used as positive controls for the S2 and NTD, respectively (Shiakolas et al., 2021). The HA-specific 3602-1707 antibody (Setliff et al., 2019.) was used as a negative control. ELISAs were performed with 2 technical duplicates and with 2 biological duplicates; data is represented as mean +/- SEM.

A

54042-4 epitope on SARS-CoV-2 S

S residue #	AA	Buried surface area
346	Arg	23
439	Asn	6
440	Asn	26
441	Leu	28
443	Ser	21
444	Lys	108
445	Val	145
446	Gly	61
447	Gly	10
448	Asn	1
449	Tyr	33
450	Asn	48
498	Gln	34
499	Pro	35
500	Thr	82

B

54042-4 paratope on SARS-CoV-2 S

	Ab residue #	AA	Buried surface area
Heavy chain	32	Ile	12
	52	Tyr	34
	53	Trp	42
	54	Asp	47
	56	Asp	42
	58	Arg	61
	97	Phe	28
	98	Ser	11
	99	Ser	99
	100A	Asp	2
	100B	Trp	2
	100C	Gly	2
Light chain	30	Phe	35
	32	Tyr	55
	91	Ser	10
	92	His	73
	93	Ser	2
	94	Thr	20
	96	Phe	6

Supplemental Figure 3: Epitope and paratope contributions to the interaction of 54042-4 to the SARS-CoV-2 RBD, related to Figure 4.

(A) SARS-CoV-2 spike residues comprising the epitope of 54042-4 are shown with their associated buried surface area ($Å^2$).

(B) 54042-4 residues comprising the antibody paratope against SARS-CoV-2 spike are shown with their associated buried surface area values ($Å^2$).

Supplemental Figure 4

A

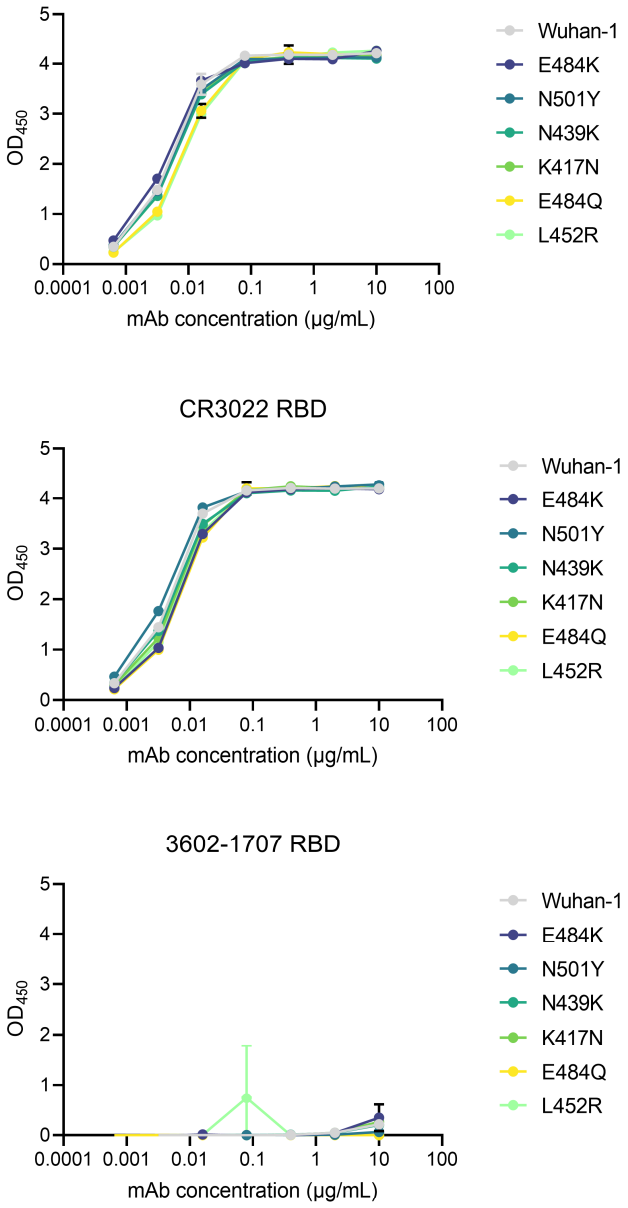

B

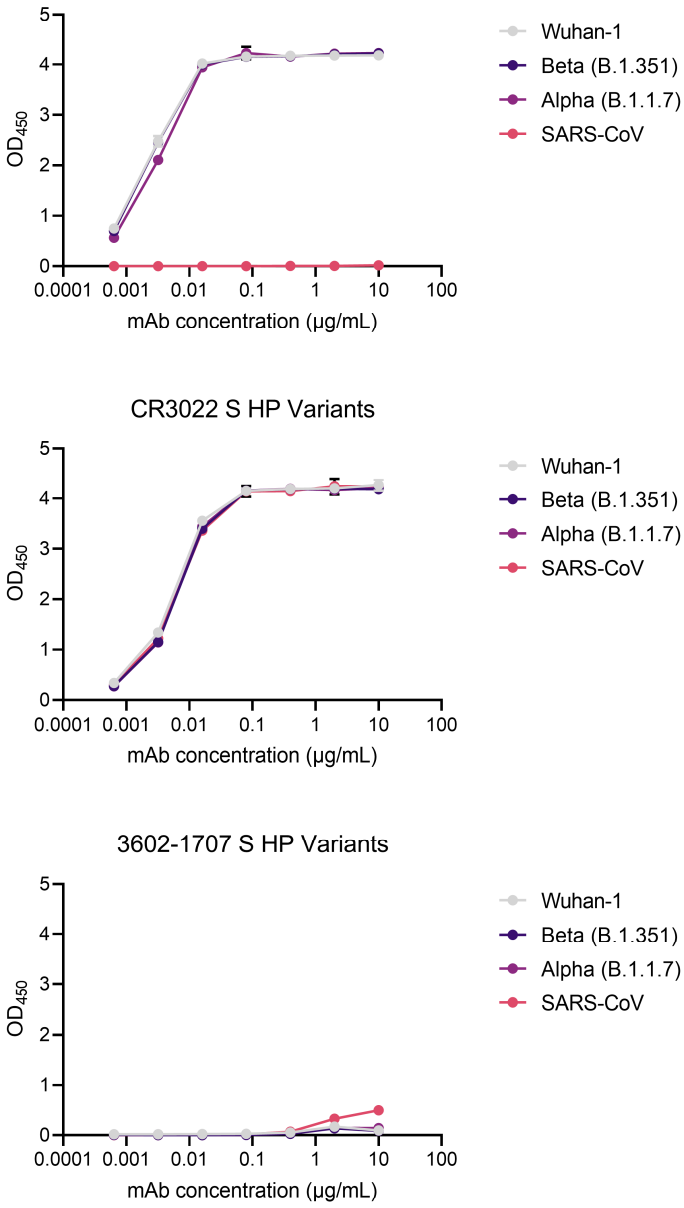

C

Mutations in S Variant Constructs

Alpha (B.1.1.7)	Beta (B.1.351)
Δ69-70	L18F
Δ144	D80A
N501Y	ΔL242-244L
A570D	R246I
P681H	K417N
	E484K
	N501Y

Supplemental Figure 4: Epitope mapping and characterization of 54042-4 binding to RBD and S1 substitutions in Alpha and Beta VOC recombinant S constructs, related to Figure 5.

(A) ELISA binding data against SARS-CoV-2 Wuhan-1 RBD and RBDs with substitutions E484K, N501Y, N439K, K417N, E484Q, or L452R. CR3022 was used as a positive control and 3602-1707, an HA-specific antibody, was used as a negative control. ELISAs were performed with 2 technical duplicates and with 2 biological duplicates; data is represented as mean +/- SD.

(B) ELISA binding data against SARS-CoV-2 S HP, SARS-CoV S, and SARS-CoV-2 S HP constructs with substitutions in the S1 domain for the Beta and Alpha variants of concern. CR3022 was used as a positive control and 3602-1707 was used as a negative control antibody. ELISAs were performed with 2 technical duplicates and with 2 biological duplicates; data is represented as mean +/- SD.

(C) The substitutions and deletions present in the Alpha and Beta SARS-CoV-2 S constructs used in the ELISAs depicted in **Supplemental Figure 4B**.

Supplemental Figure 5

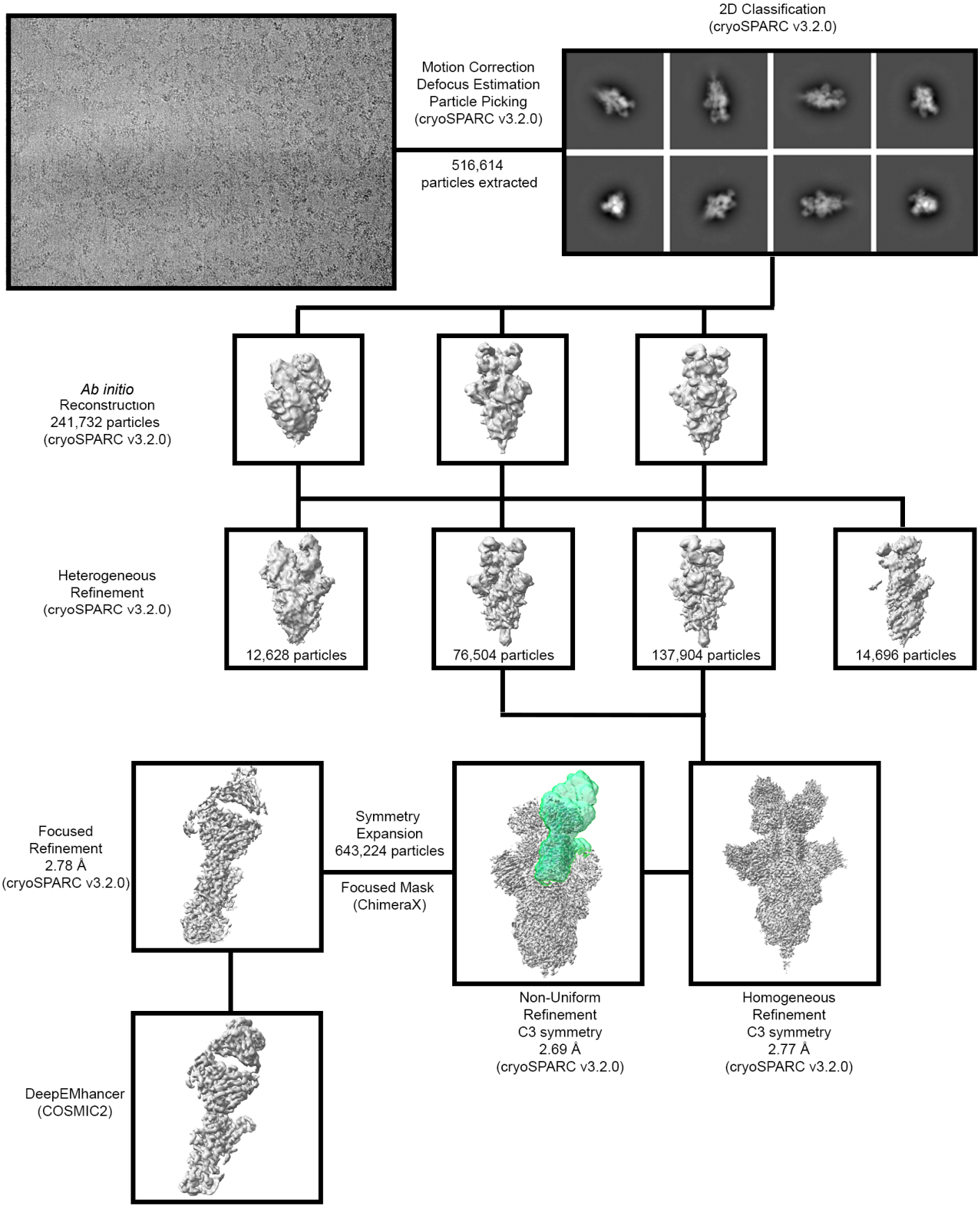

Supplemental Figure 5: Cryo-EM data processing workflow, related to Figure 3.

Flowchart outlining cryo-EM data processing of Fab 54042-4 Fab bound to SARS-CoV-2 S. Additional information can be found in the Methods section under “Cryogenic electron microscopy (cryo-EM).”

Supplemental Figure 6

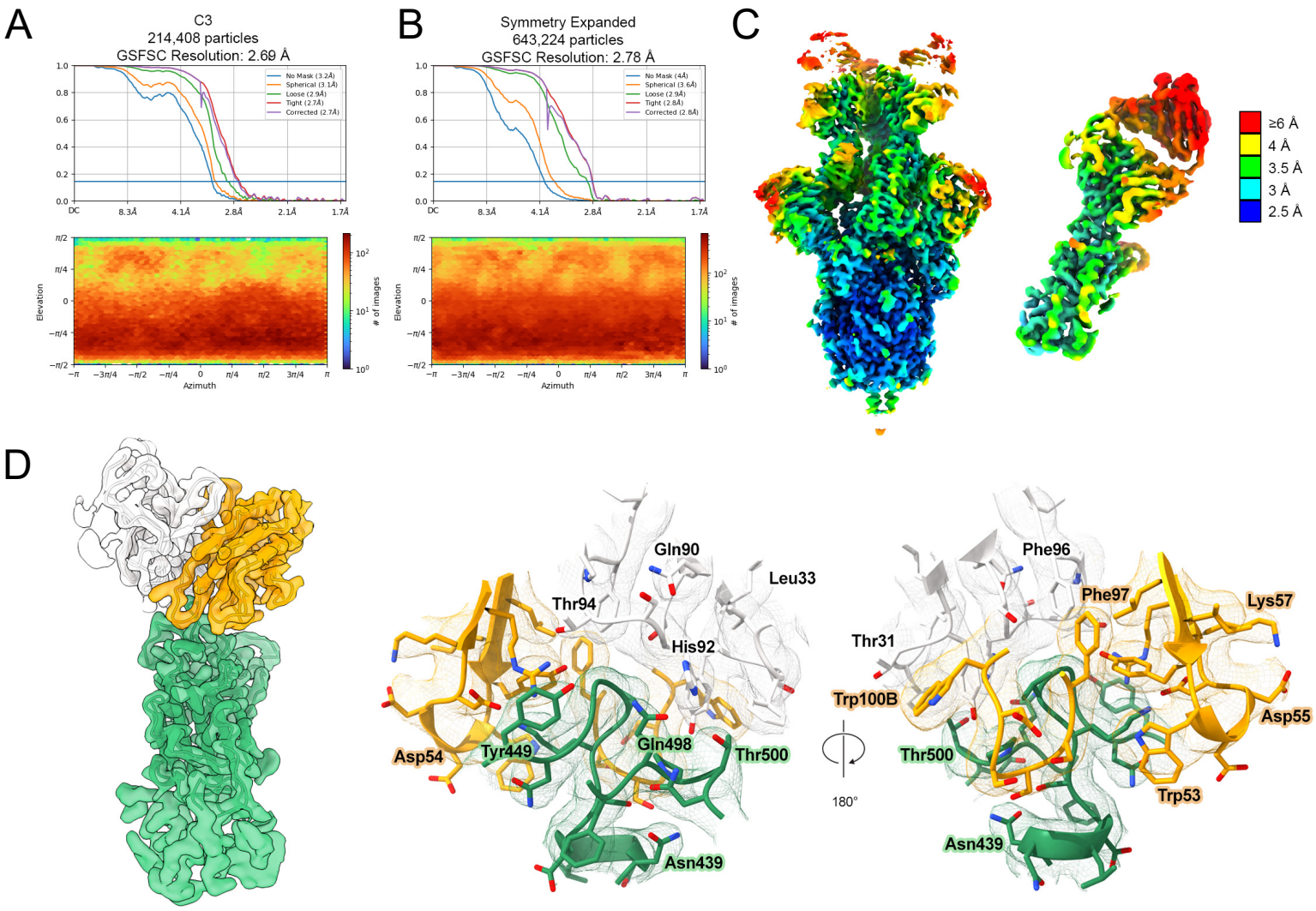

Supplemental Figure 6: Cryo-EM structure validation, related to Figure 3.

(A) FSC curve and distribution plot for the C3 S-ECD/54042-4 structure, generated in cryoSPARC v3.2.0.

(B) FSC curve and viewing distribution plot for focused refinement of the S-RBD bound to 54042-4 Fab.

(C) Local resolution shown by color of the C3 S-ECD/54042-4 (left) and focused S-RBD/54042-4 (right) reconstructions.

(D) Map resulting from focused refinement of the RBD (green) (left), 54042-4 heavy chain (orange), and 54042-4 light chain (white). Detailed views of the binding interface and corresponding map (center, right). Oxygen atoms are colored red, nitrogen blue, and sulfur yellow.

Supplemental Table 1

EM data collection	
Microscope	FEI Titan Krios
Voltage (kV)	300
Detector	Gatan K3
Magnification (nominal)	29,000
Pixel size (Å/pix)	0.81
Exposure rate (e^-/pix/sec)	9.66
Frames per exposure	100
Exposure (e^-/Å^2)	70
Defocus range (□m)	1.5-2.5
Tilt angle (˚)	30
Micrographs collected	3,762
Micrographs used	1,610
Particles extracted (total)	516,664
Automation software	SerialEM
Sample	SARS-CoV-2 S + 54042-4 Fab

3D reconstruction statistics		
	Overall	RBD-54042-4 subcomplex
Particles	214,408	643,224 (symmetry expanded)
Symmetry	C3	C1
Map sharpening B-factor	-81.8	-94.6
Unmasked resolution at 0.5 FSC (Å)	3.69	3.56
Masked resolution at 0.5 FSC (Å)	3.06	3.25
Unmasked resolution at 0.143 FSC (Å)	3.20	3.28
Masked resolution at 0.143 FSC (Å)	2.69	2.78

Model refinement and validation statistics	
Refinement package	Phenix
Refinement tool	Real-space refinement

Supplemental Table 1: PDB validation report, related to Figure 3.

EM data collection, 3D reconstruction statistics, and model refinement & validation statistics for PDB upload.

Supplemental Table 2

PDB-id	Pearson Correlation	PDB-id	Pearson Correlation	PDB-id	Pearson Correlation
6XDG	0.8543	7JMP	-0.2818	7KLG	-0.3426
7MMO	0.8483	7BEK	-0.2837	6XDG	-0.3436
7LSS	0.8251	7KFV	-0.2853	7BYR	-0.3460
7K8W	0.6007	7JX3	-0.2880	7DEU	-0.3490
7BEN	0.5747	7BEN	-0.2892	7D00	-0.3496
7L7E	0.5098	7BZ5	-0.2911	7CZR	-0.3504
7K8V	0.3231	6XKQ	-0.2918	7CWO	-0.3516
6XKP	0.1940	7BEH	-0.2946	7BEP	-0.3573
7JX3	0.1510	7CJF	-0.2976	7K9Z	-0.3586
7BWJ	0.0041	7CHB	-0.2985	7BEL	-0.3588
7CHH	-0.0111	7CZQ	-0.3023	7K8M	-0.3596
7LS9	-0.0539	7KFY	-0.3058	6XC3	-0.3604
7CZT	-0.0724	7DD8	-0.3063	7EAM	-0.3625
7K8Z	-0.1003	7K45	-0.3076	7CDI	-0.3676
7CZX	-0.1183	7D03	-0.3087	6XE1	-0.3701
7LY2	-0.1263	7B3O	-0.3126	7D0D	-0.3704
7DK4	-0.1278	7BEL	-0.3156	7LM8	-0.3743
7K8Y	-0.1519	7DPM	-0.3161	7KZB	-0.3758
7K8U	-0.1590	7NDB	-0.3172	6XC7	-0.3852
7CDJ	-0.2032	6XC3	-0.3198	7EAN	-0.3875
7K90	-0.2118	7BEI	-0.3200	7KS9	-0.3912
7L56	-0.2217	7KMI	-0.3251	7JX3	-0.3998
7L5B	-0.2261	7JMO	-0.3301	7KMH	-0.4010
7LJR	-0.2380	7CZU	-0.3303	7LAA	-0.4034
7K8S	-0.2471	7CHF	-0.3316	7JVA	-0.4056
7CZP	-0.2475	7CZY	-0.3345	7NX6	-0.4105
7JV2	-0.2565	7LM9	-0.3366	7LD1	-0.4112
7ND7	-0.2600	7NEH	-0.3370	7K9Z	-0.4178
7C01	-0.2652	7KLH	-0.3371	6XCM	-0.4192
7KMG	-0.2725	7CZV	-0.3371	7D0C	-0.4197
7CM4	-0.2796	7KFX	-0.3386	7NX8	-0.4204
6XEY	-0.2803	7ND9	-0.3393	7CH5	-0.4317
7KFW	-0.2814	7CAI	-0.3397	7L58	-0.5379

Supplemental Table 2: PDB files used for epitope comparisons, related to Figure 4.

PDB files collated to compare the angle of approach of 54042-4 to published SARS-CoV-2 RBD directed antibodies